AIAA 2003–4143

An algorithm for the recovery of 2- and 3-D BiGlobal Instabilities of Compressible Flow Over 2-D Open Cavities

V. Theofilis
Departamento de Motopropulsion y Termofluidodinámica,
E.T.S.I. Aeronáuticos, Universidad Politecnica de Madrid,
Pza. Cardenal Cisneros 3, E-28040 Madrid, SPAIN

T. Colonius
Division of Engineering and Applied Science,
California Institute of Technology,
Pasadena CA 91125, USA

33rd Fluid Dynamics Conference and Exhibit
June 23 – 26, 2003 / Orlando, FL

An algorithm for the recovery of 2- and 3-D BiGlobal Instabilities of Compressible Flow Over 2-D Open Cavities

V. Theofilis

Departamento de Motopropulsion y Termofluidodinámica,
E.T.S.I. Aeronáuticos, Universidad Politecnica de Madrid,
Pza. Cardenal Cisneros 3, E-28040 Madrid, SPAIN

T. Colonius

Division of Engineering and Applied Science,
California Institute of Technology,
Pasadena CA 91125, USA

The identification of numerical residuals from direct numerical simulations (DNS) with the least-damped BiGlobal eigenmodes of an underlying steady-state permits extraction of both the steady-state and amplitude functions of the BiGlobal eigenmodes from simple algebraic operations.[24] Algorithms for the calculation of the basic state and the spatial structure of the related BiGlobal eigenmodes from transient DNS data have been constructed and presented.

Here we extend initial calculations for the (closed) incompressible lid-driven cavity to the related (compressible) open-cavity flow. Order-of-magnitude savings are demonstrated when using of the discussed algorithm for the calculation of the basic state, compared with straightforward time-integration of the equations of motion until convergence in time. Further, employing this algorithm, different classes of instabilities in the open cavity are unified in the framework of BiGlobal instability analysis.

Nomenclature

Latin Symbols

a_∞	sound speed
D	cavity depth
$\mathsf{f_n}$	n-th mode frequency
L	cavity length
$\mathsf{L_z} = 2\pi/\beta$	periodicity length along z
Ma	Mach number
$\mathbf{q} = (\rho, \mathsf{u}, \mathsf{v}, \mathsf{p})^{\mathrm{T}}$	transient solution
$\bar{\mathbf{q}} = (\bar\rho, \bar{\mathsf{u}}, \bar{\mathsf{v}}, \bar{\mathsf{p}})^{\mathrm{T}}$	steady-state solution
$\hat{\mathbf{q}}_{2\mathrm{D}} = (\hat\rho_{2\mathrm{D}}, \hat{\mathsf{u}}_{2\mathrm{D}}, \hat{\mathsf{v}}_{2\mathrm{D}}, \hat{\mathsf{p}}_{2\mathrm{D}})^{\mathrm{T}}$	2D amplitude functions
$\tilde{\mathbf{q}} = (\tilde\rho, \tilde{\mathsf{u}}, \tilde{\mathsf{v}}, \tilde{\mathsf{w}}, \tilde{\mathsf{p}})^{\mathrm{T}}$	3D perturbations
p	pressure
Re_θ	momentum thickness Reynolds number upstream of the cavity
$\mathsf{St_n}$	Strouhal number of mode n
t	time
U	flow speed
$(\mathsf{u}, \mathsf{v}, \mathsf{w})^{\mathrm{T}}$	velocity vector components along the $(x, y, z)^{\mathrm{T}}$ coordinates
$(\mathsf{x}, \mathsf{y}, \mathsf{z})^{\mathrm{T}}$	Cartesian coordinates

Greek Symbols

β	real wavenumber parameter
θ	boundary layer (momentum) thickness
μ	viscosity
Ω	arbitrary two-dimensional domain
ω	complex eigenvalue
ω_{r}	circular frequency
ω_{i}	growth/damping
ρ	density
σ	decay rate of residuals
ψ	stream function

Subscripts

∞	ambient conditions
i	imaginary part
r	real part

The material is based upon work supported by the European Office of Aerospace Research and Development, Air Force Research Laboratory, Air Force Office of Scientific Research, under Grants No. FA8655-03-1-3059 and F49620-02-1-0362 monitored by Dr. John D. Schmisseur (AFOSR) and Mr. Wayne Donaldson (EOARD).

Introduction

Our present concern is with hydrodynamic instabilities in compressible open-cavity flows. Most theoretical work on this problem to-date has focused on a distinct feature of this flow, namely flow/acoustic resonance[15,16] through a feedback loop involving (i) excitation of an unstable shear layer, (ii) generation of an unsteady irrotational field by interaction of the shear layer with a solid boundary and (iii) the upstream influence of the irrotational field which provides for the further excitation of the instabilities in the shear layer, especially near the upstream edge. For incompressible flow, the upstream influence is instantaneous, while for compressible flow there is an acoustic delay. Resonance occurs when the phase change of a disturbance, at a given frequency, leads to constructive reinforcement and, ultimately, saturation. Because of the coupling with flow instability, cavity resonant frequencies and amplitudes may depend on the flow speed, U, the boundary layer (momentum) thickness, θ, just upstream of the cavity, ambient density, ρ_∞, viscosity, μ_∞, and sound speed, a_∞. For a two-dimensional rectangular cavity with length, L, and depth, D, there are thus 4 dimensionless parameters governing the flow $\mathsf{L/D}, \mathsf{L}/\theta, \mathsf{Re}_\theta = \rho_\infty \mathsf{U}\theta/\mu_\infty, \mathsf{Ma} = \mathsf{U}/\mathsf{a}_\infty$ as well as additional parameters and profiles that would specify the state of the boundary layer upstream of the cavity if it is turbulent. The instability mechanism proposed by Rossiter (i.e. a convectively unstable nearly parallel, two dimensional shear layer that is forced by the large acoustic field produced near the downstream interaction) is but one of several modes of instability that have been observed in flows over cavities. Factors that determine what instability mechanism will be observed include all the relevant parameters discussed above. Even for shallow cavities ($\mathsf{L/D} > 1$), Gharib and Roshko[9] observed in their incompressible experiments for an axisymmetric cavity that as the length of the cavity (relative to the upstream boundary layer thickness) was increased, there was a substantial change in the behavior of the cavity oscillations. Under these conditions, the flow was characterized by a large scale (dimensions of the cavity depth) shedding from the cavity leading edge. In two-dimensional DNS, Rowley *et al.*[17] have observed a very similar transition. In both experiment and computation, the boundary layer upstream of the cavity was laminar. The wake mode transition has also been observed in two-dimensional Reynolds-averaged Navier Stokes calculations at higher Reynolds numbers.[5,8,18] Rowley *et al.* have performed an extensive mapping of the transition to wake mode for two dimensional flows in parameter space. A key point is that the frequency of oscillation in wake mode is to be nearly constant with Mach number (from 0.4 to 0.8) and it would appear that the instability is in this regime is purely hydrodynamic in nature.

It is remarkable, indeed, that the wake mode oscillation seen in the two-dimensional simulations, is very similar to that which exists for deeper cavities that exhibit higher levels of acoustic forcing, such as the oscillations seen in gas flows in pipes with closed side branches.[13] These are high Reynolds number flows with three-dimensional turbulent flow, as well as three-dimensional geometry. While such modes have apparently not been observed in shallow cavities at high Reynolds numbers, it is at present unclear under what flow conditions the transition should occur. It is clear that three-dimensionality plays a key role. Recent Large Eddy Simulations by Shieh and Morris[18] have shown that two-dimensional cavities that are oscillating in wake mode return to the Rossiter mode when the incoming boundary layer has three-dimensional disturbances.

It is also noted that recent work by Barkley *et al.*[2] on the global linear instability of incompressible flow in the backward-facing step geometry, which can be related with that of a wide open cavity at appropriate parameter ranges, has discovered the existence of amplified large-scale small-amplitude spanwise-periodic vortical structures in this flow, which are distinct from the small-scale Tollmien-Schlichting type of instability of the shear-layer emanating from the lip of the step. This global instability is attributed to amplification of an eigenmode of the closed recirculation bubble formed between the lip and the downstream floor of the backward-facing step. An analogous mechanism has been proposed for the forward-facing step by Stuer *et al.*[20] On the other hand, two different models of closed recirculation bubbles were independently shown by Hammond and Redekopp[11] and Theofilis *et al.*[26] to support global linear instability qualitatively analogous to that of flow in the backward-facing step.

Another interesting recent observation has been made in the experimental and numerical work of Jackson *et al.*[12] in two–dimensional hypersonic closed cavity flow, where Taylor-Görtler-like vortices forming in the floor of the cavity appear to responsible for unsteadiness and three-dimensionality in the flow at low aspect ratios. As the aspect ratio increases the structure spreads and covers the entire cavity, while instability of the shear-layer only influences the laminar-turbulent transition process at very large cavity aspect ratios. The global linear instability mechanism of flow in the related lid-driven cavity model of a closed cavity flow is now well understood from a theoretical point of view[23] and also has been verified experimentally.[3] To-date such detailed investigations potentially linking the global instability which apparently exists in these related configurations and that in the open-cavity geometry have not been performed.

However, in other parameter regimes of an open cavity, modes of oscillation that exhibit features of both Rossiter mode and the wake mode have been observed.

For a cavity with $\mathsf{Ma} = 0.8$ and $\mathsf{L/D} = 0.42$ (turbulent upstream b.l.), Schlieren photographs by Forrestier *et al.*[7] show a flow structure that is clearly not describable in terms of the Kelvin-Helmholtz instability of a nearly parallel shear layer. Vortex roll up near the leading edge resembles more closely that in the early stages of the wake mode cycle, and vortical structures are ejected into the free stream to a distance above the cavity which is a significant fraction of the cavity length. DNS of two dimensional cavities shows that in an intermediate parameter regime, the flow may exhibit wake mode intermittently, with relatively quiet periods dominated by shear layer instabilities in between.

In analyzing the behavior of the shear layer, most investigators have implicitly assumed that the shear layer behavior can be described in isolation, i.e. as if it were a free shear layer. Nonparallel effects, three-dimensionality, and the coupling of the flow inside the cavity are of course neglected in such an analysis. An alternative analysis of the global instability modes, which requires spatial DNS as input, has been developed for the cavity by Theofilis.[23] The tool utilized to accomplish this task is the appropriate (in view of the inhomogeneous geometry) BiGlobal linear instability theory.[25] As in any instability analysis, the first step to be undertaken is calculation of the two-dimensional steady state. In a second step, two- and three-dimensional instabilities may be calculated by numerical solution of the appropriate partial-derivative eigenvalue problem. However, in view of the multiparametric nature of the problem indicated above, efficient tools that may circumvent the need to compute the aforementioned two-step approach are needed. Here, we discuss recovery of the steady-state and the spatial structure of damped BiGlobal eigenmodes through an algorithm originally developed for incompressible closed systems, which is readily extensible to the problem at hand.

In this paper we describe progress in the development of a unified stability theory of cavity flows. In the next section we analyze the behavior of numerical residuals near convergence towards the steady-state solution from a numerical point of view. Subsequently we discuss solutions of the partial derivative eigenvalue problem governing BiGlobal linear instability of nonparallel two-dimensional steady-state flows, which shed light on residuals from a physical viewpoint. Next, we present results obtained for the incompressible square lid-driven cavity flow problem. The link between the results of nonparallel linear instability theory and different types of behavior of numerical residuals in the DNS is demonstrated. Finally, we describe initial results in application of the algorithm to the compressible, open cavity problem.

Theory

On the phenomenology of residuals near convergence to a steady-state

While in a computation based on the steady system of equations governing fluid flow motion residuals are viewed as departure from the steady state which have to be eliminated in an efficient manner by a specific solution algorithm (e.g. multigrid), in a time-accurate integration one may view transients as solutions of the equations of motion and attempt to attach physical significance to characteristic patterns of their behavior. Here we concentrate on a time-accurate integration of the unsteady equations of motion and monitor the behavior of residuals, defined as the difference between the transient solution and the converged steady state, in flow regimes where the latter exists. Physical space is three-dimensional; without loss of generality we may take the Cartesian coordinates x and y to be defined on Ω while z denotes the third spatial coordinate in the direction of $\mathbf{\Omega}$. Along the first two coordinates the velocity vector has components u and v, while pressure is denoted by p; in compressible flow density ϱ and an equation of state complete the vector of unknowns. The equations of motion are marched in time t until $\mathbf{q} = (u, v, p)^{\mathrm{T}}$, the transient solution, converges to $\bar{\mathbf{q}}$. Assuming that the latter exists and keeping the domain Ω unchanged, the following qualitative observations are made.

First, at any Reynolds number Re at which $\bar{\mathbf{q}}$ exists, close to convergence the residuals decay exponentially in amplitude. Second, refinement of the discretization of the domain Ω at constant Re results in convergence of the rate at which the residuals decay. Third, the (converged) rate of decay of residuals is a function of the flow Reynolds number; as Re increases residuals decay slower and the associated time of integration of the equations of motion until convergence increases. Fourth, on occasion, the residuals decay at a specific constant rate for a number of decades before this rate of decay changes to a different constant value at which residuals further decay until convergence. Fifth, systematically increasing Re, instead of monotonic convergence of residuals an oscillatory behavior of $\mathbf{q}$ in the neighborhood of $\bar{\mathbf{q}}$ is observed. Ultimately, a value of Reynolds number is reached past which no $\bar{\mathbf{q}}$ exists. At first sight the existence of a physical mechanism which unifies such diverse patterns of behavior of the numerical solution seems unlikely.

A numerical point of view on the behavior of residuals near convergence

However, it is straightforward to provide an explanation of the first observation on the behavior of residuals, which also provides a handle to the link between numerical residuals and physical flow instabilities. We assume that the solution $\mathbf{q}$ is close to converging to the sought two-dimensional field $\bar{\mathbf{q}} = (\bar{u}, \bar{v}, \bar{p})^{\mathrm{T}}$ such

that it may be decomposed into the latter and small two-dimensional residuals $\tilde{\mathbf{q}}_{2D} = (\tilde{u}_{2D}, \tilde{v}_{2D}, \tilde{p}_{2D})^{\mathrm{T}}$ superimposed upon it, according to

$$\mathbf{q}(x, y, t) = \bar{\mathbf{q}}(x, y) + \varepsilon\ \tilde{\mathbf{q}}_{2D}(x, y, t), \tag{1}$$

with $\varepsilon \ll 1$. We next substitute the decomposition (1) into the continuity and Navier-Stokes equations and assume that the steady-state solution satisfies the equations of motion at $O(1)$, such that it may be subtracted out of the resulting system at this order. Subsequently, based on the smallness of the amplitude of the residuals, we linearize about $\bar{\mathbf{q}}$ and rearrange the system at $O(\varepsilon)$ such that the vector of residuals represents the unknowns; terms of $O(\varepsilon^2)$ are neglected. Since the coefficients of the resulting linear system of equations for the determination of $\tilde{\mathbf{q}}_{2D}$ at $O(\varepsilon)$ are independent of time t we may introduce an eigenmodes decomposition in this coordinate, according to

$$\tilde{\mathbf{q}}_{2D}(x, y, t) = \hat{\mathbf{q}}_{2D}(x, y)\ \mathrm{e}^{\sigma t} \tag{2}$$

with $\hat{\mathbf{q}}_{2D} = (\hat{u}_{2D}, \hat{v}_{2D}, \hat{p}_{2D})^{\mathrm{T}}$. The physical significance of the parameter σ will be discussed shortly; from a numerical point of view it represents the rate at which the residuals $\tilde{\mathbf{q}}_{2D}$ decay in the neighborhood of $\bar{\mathbf{q}}$. For simplicity we present only the real part of the admissible solutions of (2) although it is clear that both $\hat{\mathbf{q}}_{2D}$ and σ may, in general, be complex while $\tilde{\mathbf{q}}_{2D}$ is always real. Convergence of the solution $\mathbf{q}$ towards $\bar{\mathbf{q}}$ may be monitored by reference to either the local behavior of the solution $\mathbf{q}$ at a position (x_0, y_0) on Ω or by monitoring a suitably defined global criterion such as the energy contained in the residuals $\tilde{\mathbf{q}}_{2D}$; alternatives have been discussed elsewhere.[22] Here we follow the first approach and recover the parameter σ by monitoring the solution at two time-levels, $t - \Delta t$ and t, where Δt may but need not be the time-step in the numerical solution algorithm. Combining (1) and (2) it follows that the time-behavior of the solution may be monitored by

$$\sigma = \ln[\mathbf{q}^t / \mathbf{q}^{t-\Delta t}]/\Delta t \approx \mathrm{d}\ln[\mathbf{q}^{\mathrm{t}}]/\mathrm{dt}, \tag{3}$$

where

$$\mathbf{q}^t = |\mathbf{q}(x_0, y_0, t) - \bar{\mathbf{q}}(x_0, y_0)|. \tag{4}$$

The approximation in (3) holds as equality in the case of linear dependence of $\ln[\mathbf{q}^t]$ on time t. Decay of residuals is indicated by $\sigma < 0$. The first statement of the present paper is thus in place without reference to a particular flow, through the analytical result that an exponential decay of residuals near convergence should be observed as a consequence of the separability of the linearized system of equations for the determination of residuals in time.

A physical point of view based on nonparallel linear instability theory

We re-interpret the transient solution $\mathbf{q}$ in three-dimensional physical space as one composed of small-amplitude three-dimensional perturbations $\tilde{\mathbf{q}} = (\tilde{u}, \tilde{v}, \tilde{w}, \tilde{p})^{\mathrm{T}}$ superimposed upon $\bar{\mathbf{q}} = (\bar{u}, \bar{v}, \bar{w}, \bar{p})^{\mathrm{T}}$, the latter again taken to be two-dimensional. In order to simplify the presentation flow is taken to be incompressible. Linearization about $\bar{\mathbf{q}}$ is permissible on account of the smallness of perturbations compared with the steady-state $\bar{\mathbf{q}}$ and the resulting system for the determination of $\tilde{\mathbf{q}}$ is separable in both t and z on account of the steadiness and the two-dimensionality of the basic flow $\bar{\mathbf{q}}$. Eigenmodes are introduced in these directions such that

$$\tilde{\mathbf{q}}(x, y, z, t) = \hat{\mathbf{q}}(x, y)\ \mathrm{e}^{\mathrm{i}\ [\beta z - \omega t]} + c.c. \tag{5}$$

with $\hat{\mathbf{q}} = (\hat{u}, \hat{v}, \hat{w}, \hat{p})^{\mathrm{T}}$ and $\hat{w}$ being the disturbance velocity component in the z-direction. Complex conjugation is introduced in (5) since $\tilde{\mathbf{q}}$ is real while all three of $\hat{\mathbf{q}}, \beta$ and ω may be complex. In the framework of a temporal linear nonparallel instability analysis used presently we write the linearized system in the form of an eigenvalue problem for the complex quantity ω, while β is taken to be a real wavenumber parameter describing an eigenmodes in the z-direction. The real part of ω is related with the frequency of the instability mode while its imaginary part is the growth/damping rate; a positive value of $\omega_{\mathrm{i}} \equiv \Im\{\omega\}$ indicates exponential growth of the instability mode $\tilde{\mathbf{q}}$ in time t while $\omega_{\mathrm{i}} < 0$ denotes decay of $\tilde{\mathbf{q}}$ in time. In the present framework the three-dimensional space comprises Ω extended periodically in z and characterized by a wavelength L_z in this direction which is associated with the wavenumber of each eigenmode, β, through $L_z = 2\pi/\beta$.

The system for the determination of ω and $\hat{\mathbf{q}}$ takes the form of a complex nonsymmetric generalized eigenvalue problem

$$\begin{aligned}
[\mathcal{L} - (\mathcal{D}_x\bar{u})]\,\hat{u} - (\mathcal{D}_y\bar{u})\hat{v} - \mathcal{D}_x\hat{p} &= -\mathrm{i}\ \omega\ \hat{u}, && (6)\\
-(\mathcal{D}_x\bar{v})\hat{u} + [\mathcal{L} - (\mathcal{D}_y\bar{v})]\,\hat{v} - \mathcal{D}_y\hat{p} &= -\mathrm{i}\ \omega\ \hat{v}, && (7)\\
-(\mathcal{D}_x\bar{w})\hat{u} - (\mathcal{D}_y\bar{w})\hat{v} + \mathcal{L}\hat{w} - \mathrm{i}\ \beta\hat{p} &= -\mathrm{i}\ \omega\ \hat{w}, && (8)\\
\mathcal{D}_x\hat{u} + \mathcal{D}_y\hat{v} + \mathrm{i}\ \beta\hat{w} &= 0, && (9)
\end{aligned}$$

subject to appropriate boundary conditions on $\partial\Omega$. The linear operator $\mathcal{L} = (1/Re)\ \left(\mathcal{D}_x^2 + \mathcal{D}_y^2 - \beta^2\right) - \bar{u}\mathcal{D}_x - \bar{v}\mathcal{D}_y - \mathrm{i}\ \beta\bar{w}$ with $\mathcal{D}_x = \partial/\partial x$, $\mathcal{D}_x^2 = \partial^2/\partial x^2$, $\mathcal{D}_y = \partial/\partial y$ and $\mathcal{D}_y^2 = \partial^2/\partial y^2$. Some details of an efficient numerical algorithm for the solution of the matrix eigenvalue problem resulting from numerical discretization of the spatial directions x and y were discussed by Theofilis,[21] while a full discussion of the BiGlobal instability problem have been recently presented.[25]

Comparison of (1-2) and (5) reveals that the two formalisms are related in the limit $\beta \to 0$. However, $\hat{w}$ is not taken *a priori* to vanish within the framework of nonparallel linear instability; three-dimensionality of physical space is preserved and the existence of a

two-dimensional steady-state solution $\bar{\mathbf{q}}$ is the result of $\tilde{\mathbf{q}} \rightarrow 0$ as $t \rightarrow \infty$. The comparison of (1-2) and (5) highlights two further key ideas of the present paper. On the one hand, the residuals discussed earlier acquire the physical interpretation of one of the linear eigenmodes which pertain to the steady-state $\bar{\mathbf{q}}$ and have $\beta = 0$; on the other hand, the rate of decay of the residuals σ is nothing but the damping rate ω_i of this linear perturbation, as delivered by numerical solution of the partial-derivative eigenvalue problem (6-9). Another question naturally arising concerns the physical behavior of the system when the least stable member of the linear eigenspectrum which pertains to $\bar{\mathbf{q}}$ and has $\beta = 0$ becomes unstable. The answer is clearly that the existence of an unstable $(\beta = 0)-$eigenmode is mutually exclusive with the ability to obtain a converged $\bar{\mathbf{q}}$. From the point of view of the global linear instability theory based on the partial derivative eigenvalue problem (6-9) the unsteady behavior of two-dimensional flow may be related to $(\beta = 0)-$eigenmodes approaching conditions of neutral stability and interacting nonlinearly.

The answer to the second question posed in the Introduction may now also be obtained without reference to a specific flow example. The existence of a steady-state $\bar{\mathbf{q}}$ in a 2D numerical simulation is synonymous with the fact that all $(\beta = 0)-$eigenmodes of the flow have $\omega_\mathrm{i} < 0$. Modes having $\beta \neq 0$, on the other hand, may be either growing or decaying linearly. In case $\omega_\mathrm{i} < 0 \ \forall \ \beta$, a three-dimensional numerical simulation performed at some parameters in a three-dimensional domain defined by Ω and an *arbitrary* periodic extent L_z in the z-direction will deliver *identical* results for a converged $\bar{\mathbf{q}}$ compared with that of a two-dimensional simulation performed at the same parameters in the domain Ω. The situation changes in case a bracket of wavenumbers $\beta \in [\beta_1, \beta_2]$ exists which corresponds to unstable modes. The largest wavenumber β_2 defines a length $L_{z2} = 2\pi/\beta_2$; if the three-dimensional simulation is performed with $L_z < L_{z2}$ again no difference is to be expected between its result for $\bar{\mathbf{q}}$ and that of a two-dimensional simulation. Both will converge to the same steady-state solution $\bar{\mathbf{q}}$ since all wavenumbers of modes defined by an L_z constrained as above correspond to $\omega_\mathrm{i} < 0$. However, if $L_z > L_{z2}$ at least one mode in the three-dimensional simulation will be unstable, which will result in the two- and three-dimensional simulations producing different solutions.

We return to the observation of oscillatory behavior of the residuals near convergence and differentiate between exponentially decaying residuals of either sinusoidal or apparently nonlinear nature. A linear decay of $\ln[\mathbf{q}^t]$ is a consequence of $(\beta = 0)-$linear eigenmodes being stationary, i.e. having $\omega_\mathrm{r} \equiv \Re\{\omega\} = 0$. However, other stable two-dimensional member of the eigenspectrum of $\bar{\mathbf{q}}$ need not correspond to stationary modes; damped traveling modes having $\omega_\mathrm{r} \neq 0$ will manifest themselves in the time-accurate simulation as residuals of sinusoidal character the magnitude of which decays exponentially. On the other hand, the unambiguously linear dependence of $\ln[\mathbf{q}^t]$ on t in the neighborhood of $\bar{\mathbf{q}}$ is the consequence of the existence of a spectrum comprising modes which are clearly separated in parameter space from one another. The co-existence of several two-dimensional eigenmodes of approximately the same damping rate can lead to their nonlinear interaction and difficulty to observe a behavior governed by nonparallel linear instability theory. Comparison of power spectral analysis of the time-dependent DNS signal and the results of the partial-derivative eigenvalue problem (6-9) may shed light upon the two-dimensional eigenmodes involved in such a nonlinear interaction.

Recovery of the converged solution $\bar{\mathbf{q}}$ and the BiGlobal amplitude functions $\hat{\mathbf{q}}$ from transient data

Having identified small-amplitude residuals in the calculation as the least damped global two-dimensional eigenmodes of the flow, it is now possible to utilize this information in order to recover the converged steady-state solution from transient data, without having to pursue the time integration of the equations of motion until convergence in time is obtained. Combining (1), (2) and (5) one obtains

$$\mathbf{q}(x,y,t) = \bar{\mathbf{q}}(x,y) + \varepsilon \left[\hat{\mathbf{q}}_\mathrm{r} \cos\omega_\mathrm{r} t - \hat{\mathbf{q}}_\mathrm{i} \sin\omega_\mathrm{r} t\right] \mathrm{e}^{\sigma t}, \tag{10}$$

where $\hat{\mathbf{q}}_\mathrm{r} \equiv \Re\{\hat{\mathbf{q}}\}, \hat{\mathbf{q}}_\mathrm{i} \equiv \Im\{\hat{\mathbf{q}}\}$ and $\hat{\mathbf{q}}$ is one of the $(\beta = 0)-$linear eigenmodes in (5). It should be stressed here that the following discussion is applicable to transient data for which (10) holds, namely, solutions for which the entire time-dependence of the solution is exhibited in the residuals; in other words, the present analysis is based on the self-consistent premises that $\partial\bar{\mathbf{q}}/\partial t = 0$. Further, it is noted that $\hat{\mathbf{q}}$ may but need not be the least-damped member of the eigenspectrum of $\bar{\mathbf{q}}$; the only prerequisite for the validity of the following discussion is that the transient solution has reached a regime of exponential decay of residuals. A final point is that the signal near convergence need not be composed of a single damped eigenmode as (10) implies. However, the elements of the theory for the recovery of $\bar{\mathbf{q}}$ from a signal being composed of several stationary $(\omega_\mathrm{r} = 0)$ and traveling $(\omega_\mathrm{r} \neq 0)$ linearly damped eigenmodes may be exposed by reference to (10) on which we focus our attention.

The calculation of $\bar{\mathbf{q}}$ from transient data for $\mathbf{q}$ follows in two stages. First, elementary signal analysis techniques deliver the results for ω_r and σ. Second, once ω_r and σ have converged in time (10) may be used to calculate $\bar{\mathbf{q}}$. The circular frequency ω_r is calculated from the the period of oscillations in the time-signal of $\mathbf{q}$ which, in turn, is identified by the maxima in

the signal. Independently, in order to calculate σ we re-write (10) as

$$\frac{\partial^3 \mathbf{q}}{\partial t^3} + (\sigma^2 + \omega_{\rm r}^2)\frac{\partial \mathbf{q}}{\partial t} - 2\sigma\frac{\partial^2 \mathbf{q}}{\partial t^2} = 0. \qquad (11)$$

This expression may be evaluated at those times that $\partial\mathbf{q}/\partial t = 0$ in the course of the time-integration, i.e. at the same times that $\omega_{\rm r}$ is calculated. At these times the magnitude of σ is given by

$$\sigma = \frac{1}{2}\frac{(\partial^3\mathbf{q}/\partial t^3)}{(\partial^2\mathbf{q}/\partial t^2)}\Big|_{(\partial q/\partial t)=0}. \qquad (12)$$

In case $\omega_{\rm r} = 0$, a monotonic dependence of $\partial\mathbf{q}/\partial t$ on t is usually observed from the beginning of the calculation until convergence, with $\partial\mathbf{q}/\partial t = 0$ only at convergence. In this case, the magnitude of σ may be calculated using

$$\sigma = \frac{(\partial^2\mathbf{q}/\partial t^2)}{(\partial\mathbf{q}/\partial t)}. \qquad (13)$$

With σ and $\omega_{\rm r}$ converged in time (10) may be written as a linear system of three equations at three times $t_1 = t, t_2 = t+\Delta t$ and $t_3 = t+2\Delta t$ for three unknowns, $\bar{\mathbf{q}}, \hat{\mathbf{q}}_{\rm r}$ and $\hat{\mathbf{q}}_{\rm i}$ with the transient solution $\mathbf{q}_n \equiv \mathbf{q}(x, y, t_n)$ known at these times. Simple algebra delivers the desired converged steady-state solution $\bar{\mathbf{q}}$ as

$$\bar{\mathbf{q}} = \frac{\mathbf{q}_1\ {\rm e}^{2\sigma\Delta t} - 2\ \mathbf{q}_2\ {\rm e}^{\sigma\Delta t}\cos\omega_{\rm r}\Delta t + \mathbf{q}_3}{{\rm e}^{2\sigma\Delta t} - 2\ {\rm e}^{\sigma\Delta t}\cos\omega_{\rm r}\Delta t + 1}. \qquad (14)$$

The spatial structure $(\hat{\mathbf{q}}_{\rm r}, \hat{\mathbf{q}}_{\rm i})$ of the linear eigenmode $\hat{\mathbf{q}}$ may also be recovered to within an arbitrary constant from the same linear system. Equivalently, if only the converged steady-state solution is of interest, the expression

$$\bar{\mathbf{q}} = \frac{1}{\omega_{\rm r}^2 + \sigma^2}\left\{(\omega_{\rm r}^2 + \sigma^2)\mathbf{q} - 2\sigma\frac{\partial \mathbf{q}}{\partial t} + \frac{\partial^2 \mathbf{q}}{\partial t^2}\right\} \qquad (15)$$

may be used for the recovery of $\bar{\mathbf{q}}$ from transient data for $\mathbf{q}$ and its first two time-derivatives. Either of (14) or (15) may be used for the cases of residuals corresponding to stationary ($\omega_{\rm r} = 0$) or traveling ($\omega_{\rm r} \neq 0$) single linear eigenmodes.

With the steady-state solution $\bar{\mathbf{q}}$ known, the amplitude functions of the BiGlobal eigenmodes may now be calculated through

$$\hat{\mathbf{q}}_{\rm r} = \frac{s_1(\mathbf{q}_2 - \bar{\mathbf{q}}) - s_2(\mathbf{q}_1 - \bar{\mathbf{q}})}{c_2 s_1 - c_1 s_2} \qquad (16)$$

$$\hat{\mathbf{q}}_{\rm i} = \frac{c_1(\mathbf{q}_2 - \bar{\mathbf{q}}) - c_2(\mathbf{q}_1 - \bar{\mathbf{q}})}{c_2 s_1 - c_1 s_2}, \qquad (17)$$

where

$$c_1 = \exp\sigma t_1 \cos\omega_{\rm r} t_1 \qquad (18)$$

$$c_2 = \exp\sigma t_2 \cos\omega_{\rm r} t_2 \qquad (19)$$

$$s_1 = \exp\sigma t_1 \sin\omega_{\rm r} t_1 \qquad (20)$$

$$s_2 = \exp\sigma t_2 \sin\omega_{\rm r} t_2. \qquad (21)$$

The accuracy of the results delivered by (14) and (16-17) clearly depends on that by which $\omega_{\rm r}$ and σ are provided which, in turn depends on the accuracy by which the first three time-derivatives of $\mathbf{q}$ are calculated. This depends on the time-step in the calculation and the number of fields stored in order for backward differentiation formulae to be applied. Since the time-step is controlled by CFL considerations, it is advisable to store a reasonably high number of fields in order for high accuracy of $\omega_{\rm r}$ and σ and, in turn, of $\bar{\mathbf{q}}$ and $\hat{\mathbf{q}}$ to be obtained. The calculations to be presented in what follows have been performed using five-point backward differencing formulae on an equidistant grid.[1]

At conditions at which a steady-state solution exists most two-dimensional global eigenmodes of the converged steady-state are heavily damped. Consequently, if the time-integration of the equations of motion is pursued long enough, only a handful of ($\beta = 0$)−global eigenmodes will survive and persist in the DNS signal. Clearly, it is the least damped of the global instabilities that will determine the ultimate behavior of the solution. In determining whether one integrates the equations of motion until all but the least-damped of the eigenmodes have subsided in order to apply (14) or (15) or one recovers $\bar{\mathbf{q}}$ at an earlier time from a signal in which a number of damped eigenmodes still persist one should take into account the following factors.

First, the efficiency of the specific DNS algorithm determines whether the cost of integrating the equations of motion until convergence is acceptable at given flow parameters. The cost of computing $\omega_{\rm r}, \sigma$, intermediate values of $\bar{\mathbf{q}}$ and monitoring convergence of all these quantities, possibly for several eigenmodes, must also be weighed against the straightforward approach of pursuing the time-integration in the DNS until convergence. However, at all Reynolds numbers studied in the prototype flows monitored both σ and $\omega_{\rm r}$ of individual modes have converged within the first quarter to half of the total integration time, making further time-integration superfluous. While the integration time until convergence is short at low Reynolds numbers, on account of large damping rates of the least-damped linear eigenmodes, at increasingly large Reynolds numbers the magnitude of the damping rates becomes increasingly smaller and application of the ideas exposed in this section becomes increasingly attractive in order for substantial savings in computing effort to be materialized.

Results

Residuals and the ($\beta = 0$) BiGlobal eigenmode in the square lid-driven cavity

An example flow in which these ideas may be illustrated is the classic lid-driven cavity.[4] In its function as a testbed for numerous algorithms this flow has generated a substantial amount of information which is relevant to the preceding discussion. Calculations for $\bar{\mathbf{q}}$ were performed using a two-dimensional spectrally-accurate algorithm for direct numerical simulation of flow in nonperiodic geometries. The code is based on a real-space eigenvalue-decomposition of the spectral collocation differentiation matrices extending ideas discussed by Ku *et al.*[14] and uses one member of the low-storage second-order accurate time-integration schemes put forward by Spalart *et al.*[19] A spectral algorithm was chosen in order for optimal accuracy to be obtained on a low number of collocation points, the latter being dictated by the maximum number of points on which numerical solution of the partial-derivative eigenvalue problem is feasible using current computer technology. Solutions were obtained using Jacobi polynomials for the spatial discretization at resolutions depending on the Reynolds number and ranging from 32^2 to 128^2 spectral collocation points. The time-steps at the different Reynolds numbers were kept well below those dictated by the CFL condition in order for reasonable accuracy of the results of σ to be ensured.

The quality of the obtained solutions has been verified by comparing the BiGlobal instability results developing upon the steady-states obtained against benchmark calculations,[6] whereby new instability modes of the lid-driven cavity problem have been discovered.[23] Focusing on the recovery of steady-states from transient DNS data, we present in Fig. 1 the convergence histories of the two-dimensional DNS at $Re = 100, 200$ and 300, with the qualitative behavior of residuals discussed earlier observed. The convergence of the rate of decay of residuals σ, calculated using (3-4), is also shown in this figure. Additionally, the damping rate $\omega_{\rm i}$ of the least-damped $\beta = 0$ eigenmode has been calculated from numerical solution of the partial-derivative eigenvalue problem (6-9) using the converged steady-state $\bar{\mathbf{q}}$ corresponding to each Reynolds number. Excellent agreement between the two quantities has been obtained, leaves little room for doubt that numerical residuals may be identified as being the least-damped ($\beta = 0$)−eigenmode of the corresponding converged steady-state. It is interesting to note here that such an agreement could *not* be obtained when we followed the commonly-used procedure to terminate the steady-state calculation after a decay of residuals by an arbitrarily defined, seemingly adequate, small number of orders of magnitude, say 5-6. Such poorly converged in time basic states may be viewed as comprising a small unsteady component the linear instability analysis of which is bound to deliver erroneous results.

The situation becomes more intricate, but still amenable to analysis, as the Reynolds number increases. Alongside the least damped stationary mode traveling disturbances appear, as seen in the results of Fig. 1; here $\sigma(t)$ assumes the form of exponentially decaying disturbances. In order to analyze this observation we pursue two independent paths. First, we perform a nonparallel linear instability analysis of the converged steady state and monitor the least-stable member of the eigenspectrum. Second, we perform a discrete Fourier transform (DFT) of the DNS signal for $\mathbf{q}$ and compare the results with the eigenvalues of the traveling disturbances delivered by the linear instability analysis. In both this and all other moderate Reynolds number cases studied, excellent agreement between the two quantities was observed, in both the least-damped and all other members of the spectrum.

Recovery of the steady-state and the least-damped BiGlobal eigenmode from transient DNS data

Incompressible flow: the square lid-driven cavity

The preceding discussion has demonstrated the association of residuals in two-dimensional incompressible DNS calculations with the two-dimensional global linear instability modes of the converged steady state. In this section we present examples of recovery of steady-state solutions from transient DNS data using this information and the algorithm of the previous section. We stress that the applicability of the algorithm is intimately linked with the quality of the DNS results and the initial conditions used for the simulation, since both determine when, for what length of time and to which linear eigenmode the solution will be attracted in the course of the time-integration. Here we present a discussion of some parameters which affect the results returned by the algorithm in a few Reynolds number cases of those on which the algorithm was validated.

Incompressible results have been obtained in the lid-driven cavity at several Reynolds number values $Re \in [100, 7500]$, of which only those at $Re = 100$ will be presented in some detail here. At each Reynolds number three sets of calculations have been performed, two direct numerical simulations and one solution of the partial-derivative eigenvalue problem. Both DNS start from the initial condition $\psi = \zeta = 0$ for the flow streamfunction and vorticity, respectively. On the one hand, the converged 'exact' steady state $\bar{\mathbf{q}}$ has been calculated by marching the equations of motion until such a time $\bar{t}$ has been reached for the residuals to have been reduced to machine-roundoff level, using 64-bit arithmetic. On the other hand, another DNS was run but the equations of motion were marched until such a time $\bar{\bar{t}}$ was reached at which a linear regime was identified by the convergence in time of $\omega_{\rm r}$ (when applicable) and σ. The time-marching was then interrupted

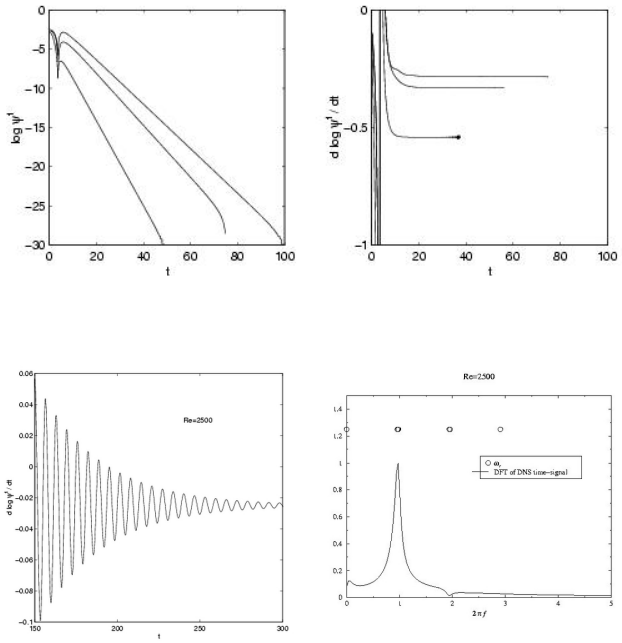

Fig. 1 Upper plot, left: Convergence history of the stream function $\psi(0.5, 0.5)$ against time. Lower to upper curves, $\mathsf{Re} = 100, 200$ and 300, respectively.[24] Right: Slopes of the respective curves. Lower plot, left: Convergence history of the stream function $\psi(\mathsf{x} = 0.5, \mathsf{y}0.5)$ against time at $\mathsf{Re} = 2500$. Right: DFT of the signal (solid line) and circular frequency ω_r (circles) of the least-damped BiGlobal eigenmodes of the converged steady-state.

and either (14) or (15) was solved for the respective 'estimated' steady-state solution $\overline{\overline{\mathbf{q}}}$. Finally, the partial-derivative eigenvalue problem (6-9) was solved for two-dimensional disturbances ($\beta = 0$) developing upon $\bar{\mathbf{q}}$ and the eigenvalue spectrum pertaining to the flow at each Reynolds number was recovered. The results were compared both in terms of the magnitude of the relative discrepancy of the two DNS-obtained solutions $\Delta\overline{\overline{\mathbf{q}}} \equiv |(\overline{\overline{\mathbf{q}}} - \bar{\mathbf{q}})/\bar{\mathbf{q}}|$ and by monitoring the difference between σ in the second set of DNS and ω_i.

Table 1 shows the resolutions and time-steps used in several simulations, the time $\bar{t}$ at which a converged steady-state solution $(\bar{\psi}, \bar{\zeta})$ was obtained by DNS and the time $\bar{\bar{t}}$ at which the damping rate of residuals converged to within a predefined tolerance of relative discrepancy 10^{-6} between successive values of σ and the results for $\overline{\overline{\psi}}$ were calculated. The value of σ as well as the relative discrepancy $\Delta\overline{\overline{\psi}} \equiv |(\overline{\overline{\psi}}(\bar{\bar{t}}) - \bar{\psi})/\bar{\psi}|$ between the estimated and the exact steady-states is also shown; the level at which the eigenmode being damped is present in the transient solution at $\bar{\bar{t}}$ may be inferred from $\Delta\psi \equiv |(\psi(\bar{\bar{t}}) - \bar{\psi})/\bar{\psi}|$.

DNS Run	I	II	III
Resolution	16×16	24×24	32×32
Δt	0.01	0.01	0.005
$\bar{t}$	50.43	50.42	49.005
$\bar{\bar{t}}$	12.71	12.79	11.07
$-\sigma$	0.540246	0.540214	0.540876
$\max(\Delta\overline{\overline{\psi}})$	$5.3(-8)$	$8.8(-7)$	$4.6(-6)$
$\min(\Delta\overline{\overline{\psi}})$	$3.6(-9)$	$7.9(-8)$	$5.1(-7)$
$\max(\Delta\psi)$	$3.4(-4)$	$3.5(-4)$	$1.0(-3)$
$\min(\Delta\psi)$	$1.5(-5)$	$1.2(-3)$	$1.6(-2)$

Table 1 Recovery of $\bar{\psi}$ in the square lid-driven cavity problem, from transient DNS data at $Re = 100$, examining the effect of resolution and time-step used in the DNS. $x(y) \equiv x \times 10^y$.

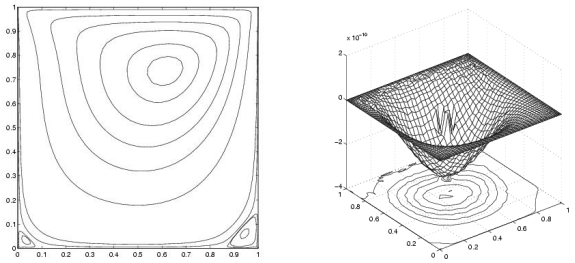

Fig. 2 Left: The approximation for $\overline{\overline{\psi}}(\mathsf{x}, \mathsf{y}; \mathsf{t} = 20)$ obtained from application of (14) to transient DNS data at $\mathsf{Re} = 100$ and $\mathsf{t} = 20$. Right: The spatial distribution of the approximation error $\Delta\overline{\overline{\psi}}(\mathsf{x}, \mathsf{y}; \mathsf{t} = 20) \equiv \overline{\overline{\psi}}(\mathsf{x}, \mathsf{y}; \mathsf{t} = 20) - \overline{\psi}(\mathsf{x}, \mathsf{y})$ at $\mathsf{Re} = 100$.

The most significant results of this table are (i) the low level of approximation error $\max(\Delta\overline{\overline{\psi}})$ and (ii) the ratio $\bar{\bar{t}}/\bar{t}$. The case $Re = 100$ is typical of one in which the least-stable eigenmode determines the transient behavior of the DNS throughout most of the time-integration process. With the results for σ converging quite quickly, the desired converged steady-state may be obtained at a time between a quarter at the coarsest and a fifth at the finest resolution of the time required by the time-marching algorithm for the residuals to be eliminated. The result for σ is only marginally affected by resolution and time-step; the precise times at which σ converges are affected by a small amount when refining the grid, with the finest resolution results converging earlier. In all cases use of the algorithm of the previous section results in substantial savings compared with the otherwise necessary computing effort.

An estimate of the converged solution $\overline{\overline{\psi}}$ obtained by application of (14) at $\bar{\bar{t}} = 15$ may be found in Fig. 2, drawn as contours at the levels of the benchmark solu-

DNS Run	I	II
Re_θ	56.9	91.0
Re_D	1500	2667
Ma	0.2	0.8

Table 2 Parameters of the DNS runs performed. In both cases $L/D = 2$.

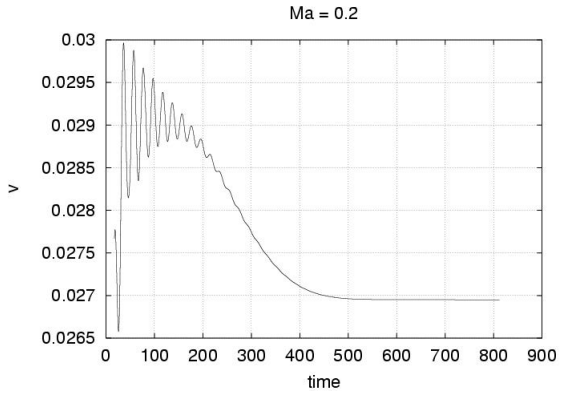

Fig. 3 Time-development of v at one location inside the open cavity.

tion.[10] No cosmetic post-processing of the results has been applied, with values presented at the collocation points used. As it is to be expected by the results of Table 1 the agreement between $\tilde{\psi}$ and the result of[10] is remarkable. The spatial distribution of the approximation error $\Delta\overline{\overline{\psi}}$, obtained using 48 collocation points to discretize each spatial direction, is also shown in Fig. 2; aside from the low level of the approximation error, it is interesting to notice that the discrepancy between the two solutions attains its maximum values in the center of the cavity and neither the singularity of the boundary conditions nor the corner vortices are manifested in this quantity. The same qualitative behavior was shown by all distributions of the approximation error at lower resolutions.

Compressible flow: the rectangular open cavity

The previous discussion is now extended to compressible open-cavity flow, where a recent detailed study, employing a well-validated high-order DNS methodology, has been presented by Rowley *et al.*[17] Results of two simulations, the parameters of which are summarized in Table 2, will be discussed in some detail.

The time-dependence of the velocity component v at a single location inside the cavity, shown in Fig 3, is characteristic of the signal returned by the DNS I for any flow quantity. Such a signal is composed of two damping BiGlobal eigenmodes, a traveling one

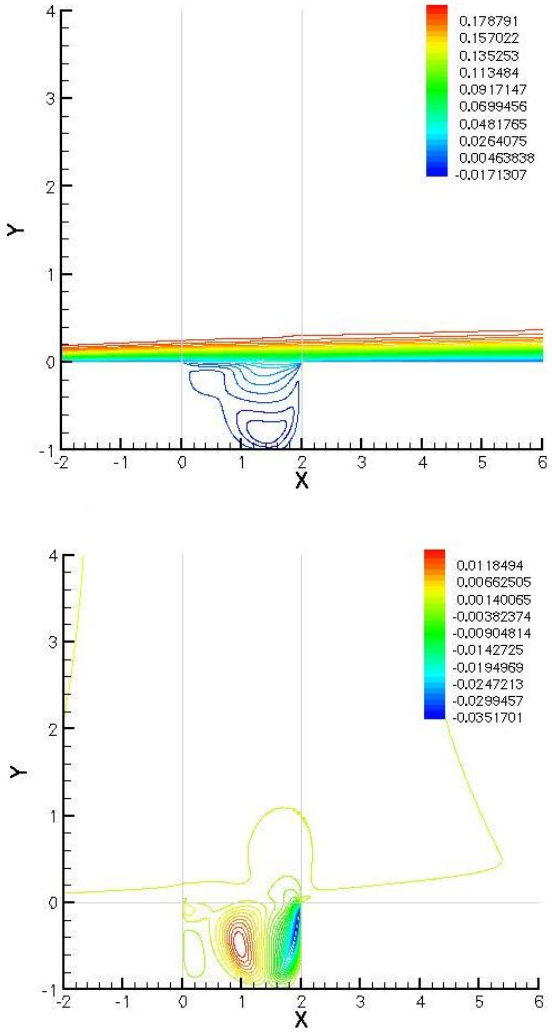

Fig. 4 The approximation of the steady-state obtained in DNS I by employing (14). Upper: $\overline{\overline{u}}$; lower: $\overline{\overline{v}}$.

visible in the signal during $t \in [0, 400]$ and a stationary one which emerges (although damped throughout the time-integration) at $t \geq 400$. Before discussing the characteristics of these modes, we first employ (14) to recover the steady state towards which the solution is converging. Fig. 4 shows the spatial distribution of the components of the velocity vector, estimated at $\overline{\overline{t}} = 600$. Compared with the exact steady state (obtained at $t = 800$) this estimate has an approximation error of $O(10^{-10})$, in line with the analogous result in the lid-driven cavity flow.

Turning to the spatial structure of the BiGlobal eigenmodes being damped in the DNS process, Figs. 5 and 6 show the amplitude functions $\hat{v}$ and $\hat{p}$ as obtained at $\overline{\overline{t}} = 100$ and 600, respectively. At $\overline{\overline{t}} = 100$ the traveling eigenmode is dominated by a Tollmien-Schlichting wave developing along the downstream cavity wall and being damped in time. At $\overline{\overline{t}} = 600$ this mode has subsided and the only remaining disturbance

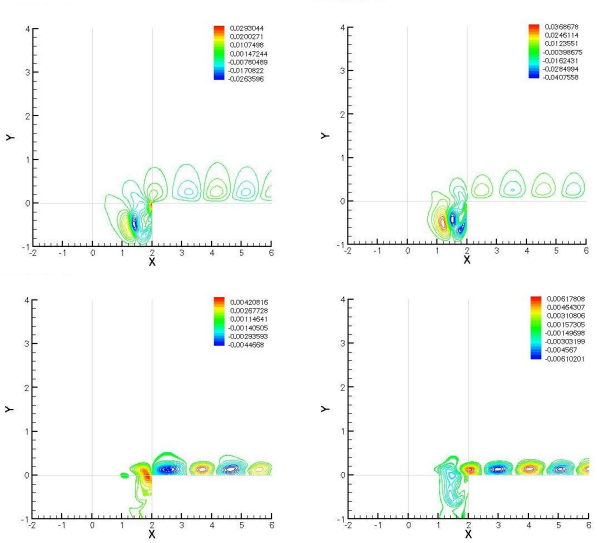

Fig. 5 Amplitude functions of $\hat{v}$ (upper row) and $\hat{p}$ (lower row) at $\bar{\bar{t}} = 100$. Left column: real parts; right column: imaginary parts.

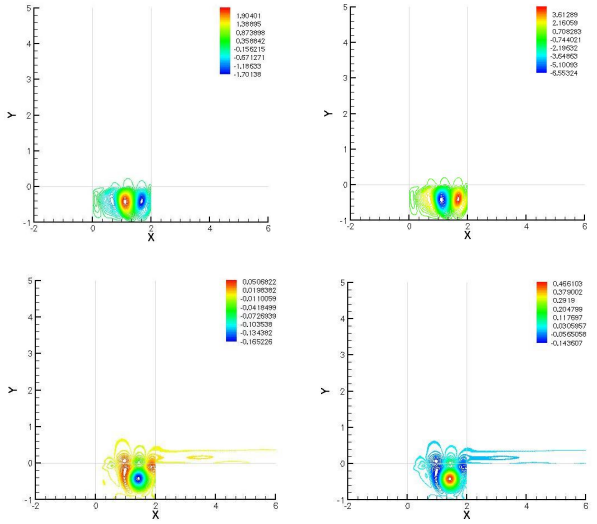

Fig. 6 Amplitude functions of $\hat{v}$ (upper row) and $\hat{p}$ (lower row) of the least-damped BiGlobal eigenmode in DNS I at $\bar{\bar{t}} = 600$.

is a stationary mode, which needs to be damped before the steady-state solution is obtained. Three properties of this mode, its being stationary, its scaling with a geometric length scale of the cavity, and its location inside the open cavity point to this BiGlobal eigendisturbance being related with the wake-mode of Gharib and Roshko.[9]

On the other hand, the spatial structure of the amplifying eigenmode manifesting itself in a linear manner at early times during DNS II has a distinctly different spatial structure of the amplitude functions. Fig. 7 also shows $\hat{v}$ and $\hat{p}$; in both results one may notice the following features. First, the dominant structure is located at the open end of the cavity and appears

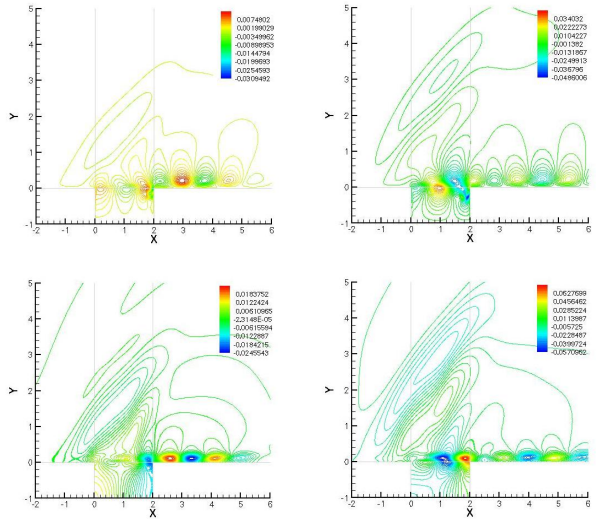

Fig. 7 Amplitude functions of $\hat{v}$ (upper row) and $\hat{p}$ (lower row) of the most-amplified BiGlobal eigenmode in DNS II at $\bar{\bar{t}} = 50$.

to be related with instability in the shear-layer, of the class predicted by the Rossiter analysis. Clearly, this disturbance is only part of the amplitude function, a significant part of which may be identified as a Tollmien-Schlichting wave on the downstream wall of the open cavity. Furthermore, weak (in comparison with the maxima of the hydrodynamic-) acoustic pressure disturbances may be identified in the respective amplitude function, apparently originating at the downstream corner of the cavity and propagating upstream in the field. The most interesting aspect of these results is that all features, which have received attention independently in the past, are part of one and the same BiGlobal flow eigenmode. Detailed discussion of the physics of these instabilities, and the effect of flow parameters on them, will be presented in future.

Conclusions

The question of differing modes of instabilities in open cavity flows may be answered within the unifying framework of the BiGlobal linear instability analysis of a two-dimensional (nonparallel) steady solution of the equations of motion.[25] Aided by the results of a numerically well-studied incompressible flow problem we were able to attach physical significance to the transient behavior of two-dimensional time-dependent incompressible direct numerical simulation results. What is commonly known as residual in the simulation is either the least damped two-dimensional ($\beta = 0$) linear eigenmode of the converged steady state itself, or can be related to a small number of the least damped modes of the full eigenvalue spectrum. The physical information which is suppressed in two-dimensional simulations based on the steady formulation of the equations of motion concerns the

dynamical behavior of these two-dimensional linear eigenmodes.

When a steady-state solution exists, the insight gained from the association of the transient behavior of residuals in two-dimensional DNS with the results of the nonparallel linear instability analysis of the converged steady-state may be used in a threefold manner. First, an algorithm may be constructed, to recover the steady-state solution from transient data taken well before convergence, thus making further time-integration of the equations of motion redundant. The algorithm is based on identification of the parameters pertaining to the linear eigenmodes which determine the transient behavior of the solution, namely the damping rate $\sigma \equiv \omega_{\mathrm{i}}$ and the frequency ω_{r} of the least stable eigenmodes. Results presented have demonstrated that up to three-quarters of the otherwise necessary effort to compute the steady-state may be saved by application of the theory presented herein. Second, the results of a nonparallel linear instability analysis of the converged steady-state can be used as a quality test of the obtained solution, if the latter has been obtained using a time-accurate solution approach. The rate of decay of the residual which ultimately has to be damped in order for a converged steady-state to be obtained should equal the damping rate of the least-stable eigenmode. Disagreement of these two quantities indicates that the obtained steady-state still contains an unsteady component which must be eliminated by further time-integration*. Third, the spatial structure of the least damped BiGlobal eigenmode may be computed from the same transient DNS data. In this manner solution of the partial-derivative eigenvalue problem (6-9) may be circumvented.

The first application of this algorithm to an open-flow problem, that of compressible (subsonic) flow in an aspect-ratio 2 open cavity has been presented. In this flow too, accurate predictions of the steady-state can be delivered and the spatial structure of the most energetic members of the BiGlobal eigenspectrum may be recovered. In view of its essentially inhomogeneous nature, the wake-mode instability may be studied in the framework of BiGlobal instability analysis. Furthermore, hydrodynamic (shear-layer, Tollmien-Schlichting) and aeroacoustic instabilities in open cavities may be re-interpreted as components of the amplitude function of *single* BiGlobal eigenmodes, a realization which opens new modeling avenues.

*or by application of the theory discussed herein

References

[1]M. Abramowitz and I. Stegun. *Handbook of mathematical functions*. Dover, 1970.

[2]D. Barkley, G. Gomes, and R.D. Henderson. Three-dimensional instability in flow over a backward facing step. *J. Fluid Mech.*, 1998. (submitted).

[3]J. D. Benson and C. K. Aidun. Transition to unsteady non-periodic state in a through-flow lid-driven cavity. *Phys. Fluids* A, 4:2316–2319, 1992.

[4]O. R. Burggraf. Analytical and numerical studies of the structure of steady separated flows. *J. Fluid Mech.*, 24:113–151, 1966.

[5]A. Cain, Rubio A. D., D. M. Bortz, H. T. Banks, and R. C. Smith. Optimizing control of open bay acoustics. AIAA Paper 2000-1928, 2000.

[6]Y. Ding and M. Kawahara. Linear stability of incompressible flow using a mixed finite element method. *J. Comput. Phys.*, 139:243–273, 1998.

[7]N. Forestier, P. Geffroy, and L. Jacquin. Etude expérimentale des propriétés instationnaires d'une couche de mélange compressible sur une cavité: cas d'une cavité ouverte peu profonde. Technical Report RT 22/00153 DAFE, ONERA, 2000.

[8]D.F. Fuglsang and A.B. Cain. Evaluation of shear layer cavity resonance mechanisms by numerical simulation. AIAA Paper 92-0555, 1992.

[9]M. Gharib and A. Roshko. The effect of flow oscillations on cavity drag. *J. Fluid Mech.*, 177:501–530, 1987.

[10]U. Ghia, K. N. Ghia, and C. T. Shin. High-Re solutions for incompressible flow using the Navier-Stokes equations and a multigrid method. *J. Comput. Phys.*, 48:387–411, 1982.

[11]D. A. Hammond and L. G. Redekopp. Local and global instability properties of separation bubbles. *Eur. J. Mech. B/Fluids*, 17:145–164, 1998.

[12]A. P. Jackson, R. Hillier, and S. Soltani. Experimental and computational study of laminar cavity flows at hypersonic speeds. *J. Fluid Mech.*, 427:329–358, 2001.

[13]P. C. Kriesels, M. C. A. M. Peters, A. Hirshberg, A. P. J. Wijnands, A. Iafrati, G. Riccardi, R. Piva, and J. C. Bruggeman. High aplitude vortex-induced pulsations in a gas transport system. *Journal of Sound and Vibration*, 184(2):343–368, 1995.

[14]H. C. Ku, R. S. Hirsch, and T. D. Taylor. A pseudospectral method for solution of the three-dimensional incompressible Navier-Stokes equations. *J. Comput. Phys.*, 70:549–462, 1987.

[15]A. Powell. On the edgetone. *J. Acous. Soc. Am.*, 33:395, 1961.

[16]J. E. Rossiter. Wind-tunnel experiments on the flow over rectangular cavities at subsonic and transonic speeds. Aeronautical Research Council Reports and Memoranda, No. 3438, October 1964.

[17]C. Rowley, T. Colonius, and A. Basu. On self-sustained oscillations in two-dimensional compressible flow over rectangular cavities. *J. Fluid Mech.*, 455:315–346, 2002.

[18]C. M. Shieh and P. J. Morris. Parallel computational aeroacoustic simulation of turbulent subsonic cavity flow. AIAA Paper 2000-1914, 2000.

[19]P. R. Spalart, R. D. Moser, and M. M. Rogers. Spectral methods for the Navier-Stokes equations with one infinite and two periodic directions. *J. Comput. Phys.*, 96:297–324, 1991.

[20]H. Stüer, A. Gyr, and W. Kinzelbach. Laminar–turbulent transition of a separatin flow on a forward facing step. In W. Saric and H. Fasel, editors, *Proc. of the IUTAM Laminar-Turbulent Symposium V*, pages 541–546, Sedona, AZ, USA, 2000.

[21]V. Theofilis. Linear instability in two spatial dimensions. In K. D. Papailiou, editor, *Fourth European Computational Fluid Dynamics Conference ECCOMAS'98*, pages 547–552, Chichester, N. York, 1998. J. Wiley and Sons.

[22]V. Theofilis. On linear and nonlinear instability of the incompressible swept attachment-line boundary layer. *J. Fluid Mech.*, 355:193–227, 1998.

[23]V. Theofilis. Globally-unstable flows in open cavities. page 12 pp. AIAA Paper 2000-1965, 2000.

[24]V. Theofilis. On steady–state flow solutions and their nonparallel global linear instability. In C. Dopazo, editor, 8^{th} *European Turbulence Conference, June 27–30, 2000*, pages 35–38, Barcelona, Spain, 2000.

[25]V. Theofilis. Advances in global linear instability of nonparallel and three-dimensional flows. *Prog. Aero. Sciences*, 39 (4):249–315, 2003.

[26]V. Theofilis, S. Hein, and U.Ch. Dallmann. On the origins of unsteadiness and three-dimensionality in a laminar separation bubble. *Phil. Trans. Roy. Soc. London (A)*, 358:3229–3246, 2000.